Astron. Astrophys. 249, 474–482 (1991)

ASTRONOMY AND ASTROPHYSICS

Formation of dust grains in the ejecta of SN 1987A. II

T. Kozasa[1], **H. Hasegawa**[2], **and K. Nomoto**[3]

[1] Max-Plank-Institut für Kernphysik, W-6900 Heidelberg 1, Federal Republic of Germany
[2] Department of Liberal Arts, Osaka Sangyo University, Osaka 574, Japan
[3] Department of Astronomy, University of Tokyo, Tokyo 113, Japan

Received August 31, 1990; accepted March 2, 1991

Abstract. Observations have confirmed the formation of dust grains in the metal-rich ejecta of SN 1987A. In this paper the grain formation in the ejecta is reinvestigated on the basis of the revised hydrodynamical model and elemental composition of the ejecta, and of the theory of homogeneous nucleation and grain growth.

The adopted abundance distribution in the ejecta, inferred from the behavior of the bolometric light curve around its maximum and the early emergence of X-rays and γ-rays, results in the sequential formation of Al_2O_3, $MgSiO_3$ and Fe_3O_4 grains respectively in the ejecta at $1.0\ M_\odot \leq M_r \leq 4.4\ M_\odot$ as the gas cools down. In the inner region at $M_r \leq 1.0\ M_\odot$, on the other hand, the latent heat deposited during the grain growth retards the formation of dust grains. The observed enhancement of 10 μm flux at ~day 465 after the explosion being assigned to the thermal radiation from Al_2O_3 grains formed in the ejecta, $MgSiO_3$ grains start to form at ~day 550, and Fe_3O_4 grains at ~day 620, and the grains cease to form at ~day 730 in the region at $1.0\ M_\odot \leq M_r \leq 4.4\ M_\odot$. The total mass of dust grains formed in this region is $\sim 0.23\ M_\odot$. The radii of grains newly formed in the ejecta are typically ~10 Å for Al_2O_3 and Fe_3O_4, and ~70 Å for $MgSiO_3$ grains.

The calculated grain radius smaller than 0.01 μm satisfies the constraint on the grain size in the ejecta imposed by the analysis of the blue-shifted optical lines. Comparing the observed infrared light curve with the calculated one based on both the condensation calculation and the observed 10 μm flux, we suggest that: 1) The condensation efficiency of dust grains in the ejecta is greater than 0.3, or the clumps occupies the fraction of at least ~20% of the ejecta on the average. 2) The grain number density in the clumps is less than 5 times that of the uniform ejecta. 3) The observed infrared luminosity is attributed to the thermal radiation from dust grains in the optically thick part of the ejecta.

Key words: supernovae: individual (SN 1987A) – dust grains: formation – infrared radiation

1. Introduction

SN 1987A, discovered on Feb. 23 1987 in the Large Magellanic Cloud, has given us a great deal of new information about the stellar evolution, nucleosynthesis of massive stars, mechanism of supernovae explosions, and physical and chemical evolution of the ejecta. The recent observations in particular have confirmed the formation of dust grains in the ejecta (Whitelock et al. 1989; Moseley et al. 1989; Danziger et al. 1989; Lucy et al. 1989, 1991; Wooden 1989; Suntzeff & Bouchet 1990), which had not been clear for distant extragalactic supernovae (Dwek 1983; Dwek et al. 1983).

The observations relevant to the grain formation in the ejecta are summarized as follows:

1) The infrared observations have confirmed the enhancement of 10 μm flux starting from ~day 465 (Roche et al. 1989). This infrared excess can be attributed to the thermal radiation from dust grains formed in the ejecta (Kozasa et al. 1989b), although it cannot rule out the possibility that a part of this flux might have been due to the infrared light-echo arising from the circumstellar materials (Roche et al. 1989; Smith 1989). The time variation of [Mg I] line intensity (Lucy et al. 1991) and the fluctuation of U and B light curves (Burki et al. 1989) have also suggested the onset of grain formation in the ejecta at ~day 450.

2) The observed U to M bolometric luminosity together with X-rays and γ-rays flux have deviated from that expected from the decay of radioactive elements from ~day 500, which concurrently occurred with the enhancement of 10 μm flux (Whitelock et al. 1989). This behavior of the bolometric light curve can be interpreted self-consistently in terms of the decay of the radioactive elements ^{56}Co and ^{57}Co when adding the observed mid- to far-infrared luminosity to the U to M bolometric luminosity (Whitelock et al. 1989; Moseley et al. 1989; Suntzeff & Bouchet 1990). This result, which cannot be explained by the infrared-echo model, thus strongly supports the argument that the observed mid- to far-infrared radiation can be attributed to the thermal radiation from dust grains formed in the ejecta (Whitelock et al. 1989). The grain formation in the ejecta has been also suggested from the change in the decline rate of U, B and V magnitude beginning at ~day 500 and the change in $V-K$ color suddenly occurred at ~day 500 (Suntzeff & Bouchet 1990).

3) Blue-shifted profiles of [Mg I], [O I], [C I] and [Si I] lines (Danziger et al. 1989; Lucy et al. 1989), and the concurrent decrease in the intensities of [Mg I], [O I] and [Si I] lines have been observed from ~day 530 (Lucy et al. 1991). These blue-shifted line profiles are interpreted as a result of the attenuation of line emission from the receding shell by the dust grains which are uniformly distributed in the ejecta (Lucy et al. 1989, 1991).

Send offprint requests to: T. Kozasa

The theoretical investigations have predicted the possibility of the formation of dust grains in the ejecta of SN 1987A (Dwek 1988; Kozasa et al. 1989a). In forming dust grains, the elemental composition and the time variation of gas density and temperature in the ejecta are crucial in determining when, what type of and what sizes of dust grains form in the ejecta (Kozasa et al. 1989a). Moreover, the large-scale mixing and the clumping in the ejecta as suggested from observational and theoretical studies would affect the process of grain formation and the resulting thermal radiation from newly formed grains.

In this paper we reinvestigate the grain formation in the ejecta of SN 1987A on the basis of the revised hydrodynamical model and elemental composition in the ejecta; the revised model reproduces well the behavior of the bolometric light curve around its maximum and the early emergence of X-rays and γ-rays. The condensation calculation is based on the theory of homogeneous nucleation and grain growth in order to clarify when, what type of, and what sizes of dust grains form in the ejecta of SN 1987A. The elemental composition and the process of grain formation in the ejecta are summarized in Sect. 2. The result of calculations of the formation of Al_2O_3, $MgSiO_3$, and Fe_3O_4 grains in the ejecta is presented in Sect. 3. The condensation efficiency of dust grains and the degree of the clumping of the ejecta are discussed in comparison with the observations in Sect. 4. The concluding remarks are presented in Sect. 5.

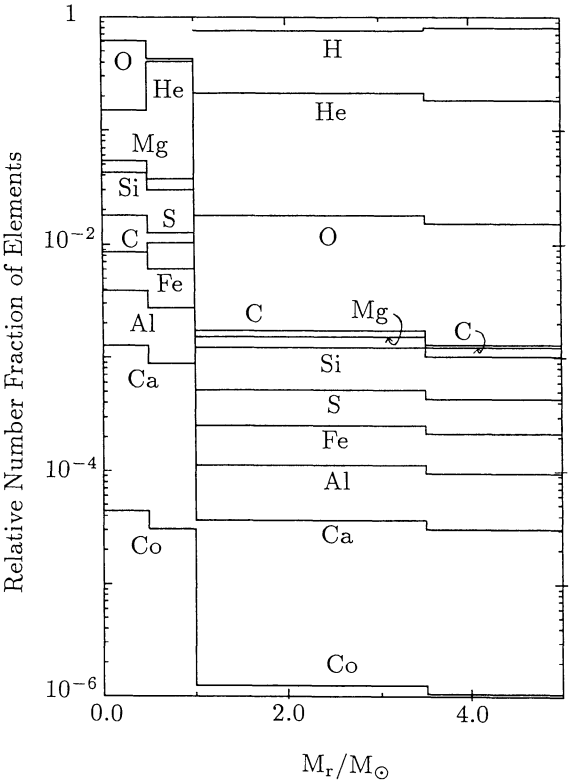

Fig. 1. The distribution of elements which are of interest to the grain formation in the ejecta at day 600 after the explosion, where the decay of ^{56}Co to ^{56}Fe is taken into account

2. The elemental composition and the grain formation in the ejecta

The condensation time, radius and number density of dust grains formed in the ejecta depend on the manner in which the gas density and temperature vary with the expansion of the ejecta. The elemental composition in the ejecta determines what type of grains form. The process of grain formation is treated by a theory of homogeneous nucleation and grain growth (Yamamoto & Hasegawa 1977; Draine & Salpeter 1977; Kozasa & Hasegawa 1987; Hasegawa & Kozasa 1988).

The hydrodynamical model of the ejecta adopted here is based on the progenitor model 14E1 by Shigeyama & Nomoto (1990), where the ejecta mass is 14.6 $M_\odot$ and the final kinetic energy of explosion is $1\,10^{51}$ erg. The inner 2 $M_\odot$ region is subject to explosive processing (Hashimoto et al. 1989; Thielemann et al. 1990). The ejecta is composed of 4.4 $M_\odot$ He + metal-rich core and 10.2 $M_\odot$ hydrogen-rich envelope. Here we consider the formation of dust grains in the metal-rich ejecta, i.e., in the region of the inner 4.4 $M_\odot$.

For the elemental composition in the ejecta, Shigeyama & Nomoto (1990) have claimed that hydrogen in the outer envelope has been mixed into the inner region down to 1 $M_\odot$ in order to realize the behavior of bolometric light curve around its maximum at ~day 80. Moreover, the mixing of radioactive element ^{56}Co as well as heavy elements from the inner-most region into the outer envelope explains the early emergence of X-rays and γ-rays (Kumagai et al. 1989 and references therein). The resulting elemental composition which is of interest to the grain formation in the ejecta is shown in Fig. 1, where we adopt the relative number abundance at day 600, taking account of the decay of ^{56}Co into ^{56}Fe. Further we assume that the mass abundance of Al is 0.0107 times that of O, referring to the result of explosive nucleosynthesis calculation (Thielemann et al. 1990).

The treatment of the process of grain formation in the ejecta is the same as that of the previous paper (Kozasa et al. 1989a, hereafter referred to as Paper I), which is based on the theory of homogeneous nucleation and grain growth (Kozasa & Hasegawa 1987). It should be noted that the theory is based on a classical nucleation theory, the rate constants of chemical reactions at the time of nucleation and grain growth are assumed to be equal, and that the condensates are considered to be minerals which are stable ones thermodynamically in a given physical condition. There are controversies for the application of classical homogeneous nucleation theory to the formation of refractory grains (Donn & Nuth 1985), while it is also true that there is no alternative theory in order to understand comprehensively the process of grain formation in astrophysical environments.

The time variation of gas density and temperature in the ejecta is crucial in considering the process of grain formation. In the ejecta the gas density at a location of a given M_r decreases as $\rho(t) \propto t^{-3}$ after the shock wave reaches the surface of progenitor. On the other hand, the gas temperature in the ejecta is controlled by various types of heating and cooling mechanisms: The heating is due to the collision with photons and electrons resulting from the Compton degradation of γ-rays from the decay of radioactive elements, and the cooling due to emission from atoms and molecules. Instead of calculating these complicated heating and cooling processes exactly, we assume that the gas temperature decreases as $T(t) \propto t^{-3(\gamma-1)}$ after the gas passes through the photosphere. Then the gas density $\rho(t)$ and temperature $T(t)$ after the gas passes through the photosphere are given by $\rho(t) = \rho_p (t/t_p)^{-3}$ and $T(t) = T_p (t/t_p)^{-3(\gamma-1)}$, respectively. The time t_p at which the gas passes through the photosphere as well as the gas

temperature T_p and density ρ_p at the photosphere can be evaluated by combining the photometric observations (Catchpole et al. 1987, 1988) with the hydrodynamical model of the ejecta (Shigeyama & Nomoto 1990). Figure 2 shows the time t_p and the gas temperature T_p for the gas at given locations in the ejecta; see Shigeyama & Nomoto (1990) for the gas density. The parameter γ is assumed to be a constant throughout the ejecta. Then we can derive the quantities that characterize the process of homogeneous nucleation and grain growth. As pointed out in Paper I, the condensation time of dust grains in the ejecta strongly depends on the value of γ, so that we may be able to estimate the value of γ precisely by comparison with the observations rather than with theoretical studies.

Here we must keep in mind the followings: In the ejecta filled with condensable elements as well as heavy elements (see Fig. 1), the latent heat deposition during the grain growth may raise up the grain temperature high enough to evaporate the grains nucleated. We define the *stabilization time* t_{stat} as a time after which the grains can grow stably against the spontaneous latent heat deposition. In the followings we refer to the *condensation time* t_{con} when the time determined by the process of homogeneous nucleation and grain growth is larger than the *stabilization time* (see Paper I for the details), where we assume that the latent heat is carried away through collision with gas and that the thermal accommodation coefficient is unity. Generally lighter gaseous species collide frequently with dust grains and can carry away the latent heat deposited during the grain growth. In relation with the condensation process described above, the major difference from the uniformly mixed ejecta discussed in Paper I is that in the elemental distribution of the ejecta adopted here hydrogen is intruded to the region down to $M_r = 1.0\ M_\odot$.

3. Result of calculations

In the following calculations we assume all C and Si atoms are locked up into CO and SiO molecules respectively at the time when nucleation occurs, since the ejecta is oxygen rich as seen from Fig. 1. These molecules in the ejecta have been detected by the infrared observations (Danziger et al. 1988). The elemental composition in the ejecta (Fig. 1) then leads to the formation of Al_2O_3, $MgSiO_3$ and Fe_3O_4 grains as major species. The choice of $MgSiO_3$ as the silicate grains instead of Mg_2SiO_4 is due to the fact that the Mg/Si ratio is ~ 1 in the number fraction, and this is different from Paper 1.

Let us assign the day 465 to the time at which the grains begin to condense in the ejecta by referring to the observed enhancement of 10 μm flux at ~day 465 after the explosion (Roche et al. 1989). We can then determine the value of unknown parameter γ so that one species of dust grains can start to condense at ~day 465. Al_2O_3 grain is the first condensate of all grain species in the ejecta with the elemental composition of Fig. 1; it starts to condense at ~day 460 when we adopt the value of $\gamma = 1.27$. In what follows, we consider the formation of dust grains in the ejecta with $\gamma = 1.27$.

Figure 3 shows the time variation of the gas temperature in the ejecta after the explosion, which is calculated by the procedure described in Sect. 2. The gas is almost isothermal at a given time in the region at $1.7\ M_\odot \leq M_r \leq 4.4\ M_\odot$. In the inner region at

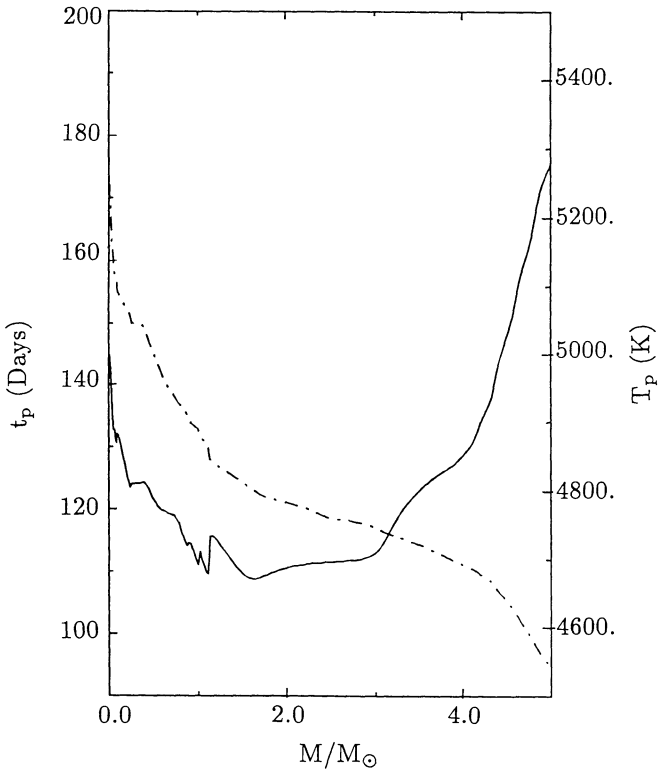

Fig. 2. The time t_p at which a gas passes through the photosphere and the gas temperature T_p at given locations in the ejecta. The dash-dotted curve is for t_p and the solid curve for T_p

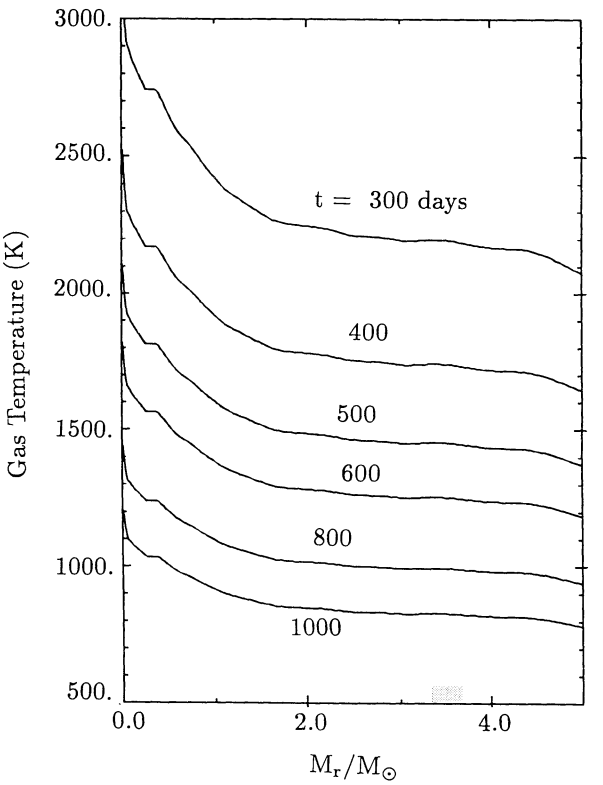

Fig. 3. The gas temperature distribution in the ejecta with $\gamma = 1.27$ at the given times after the explosion

$M_r \leq 1.7\ M_\odot$, the gas temperature increases gradually toward the inner region, which reflects the gradual decrease in the expansion velocity toward the inner region.

In the region at $1.0\ M_\odot \leq M_r \leq 4.4\ M_\odot$, hydrogen and helium atoms are abundant enough to carry away the latent heat released during the grain growth; then each dust grain is formed via the process of homogeneous nucleation and grain growth. The *condensation times* are represented by the solid curves in Fig. 4. As the gas cools down, Al_2O_3 grains condense at $1.0\ M_\odot \leq M_r \leq 4.4\ M_\odot$ starting from ~day 460 up to day 540, $MgSiO_3$ grains from ~day 550 to day 640, and Fe_3O_4 grains from ~day 620 to day 730. Each grain species condenses almost simultaneously throughout the region at $1.7\ M_\odot \leq M_r \leq \sim 4.0\ M_\odot$: Al_2O_3 grains at ~day 470, $MgSiO_3$ grains at ~day 560, and Fe_3O_4 grains at ~day 630. This reflects the fact that the gas temperature in this region is almost spatially constant as shown in Fig. 3. Note that Mg-silicate can condense in this region via the process of homogeneous nucleation and grain growth; this is in contrast to the case of uniformly mixed ejecta discussed in Paper I, where the latent heat deposition greatly retards the formation of Mg-silicate grains.

In the inner region at $M_r \leq 1.0\ M_\odot$, on the contrary, the grains nucleated cannot grow stably against heating due to the latent heat deposition during the grain growth: This is (1) because condensable elements deposit much latent heat, and (2) because the lighter elements are too low in abundance to carry away efficiently the deposited latent heat. The effect of the latent heat deposition on the formation of dust grains becomes prominent in the order of Al_2O_3, Fe_3O_4, and $MgSiO_3$. The *stabilization times* of Al_2O_3 and Fe_3O_4 grains, which are shown by the dotted curves in Fig. 4, are respectively at the longest ~100 days and ~150 days after the condensation time determined by the process of homogeneous nucleation and grain growth. The effect of the latent heat deposition on the formation of $MgSiO_3$ grains is most prominent. Accordingly the formation of $MgSiO_3$ grains would not be expected because the gas density is too low to complete the grain growth in the region where the grains can grow stably against the effect of the latent heat deposition.

Figure 5 shows the final radii of each grains formed at $1.0\ M_\odot \leq M_r \leq 4.4\ M_\odot$. In this region, dust grains forming via the process of homogeneous nucleation and grain growth grow up to the final sizes soon after t_{con}. The final grain radius is approximately proportional to the concentration of the key molecular species at t_{con}. The radii of Al_2O_3 and Fe_3O_4 grains are typically ~10 Å, and the radius of $MgSiO_3$ grains is ~70 Å, reflecting the differences in both the abundances of key molecular species and the t_{con}. The hump of each grain radii around $M_r = 2\ M_\odot$ reflects the hump of gas density in the ejecta.

4. Discussion

The result of our calculations shows that the condensation of dust grains starts at ~day 460 and continues up to ~day 730 at the region of $1.0\ M_\odot \leq M_r \leq 4.4\ M_\odot$. This duration of the condensation episode in the ejecta is comparable to that derived from the analysis of blue-shifted line profiles (Lucy et al. 1989, 1991) and

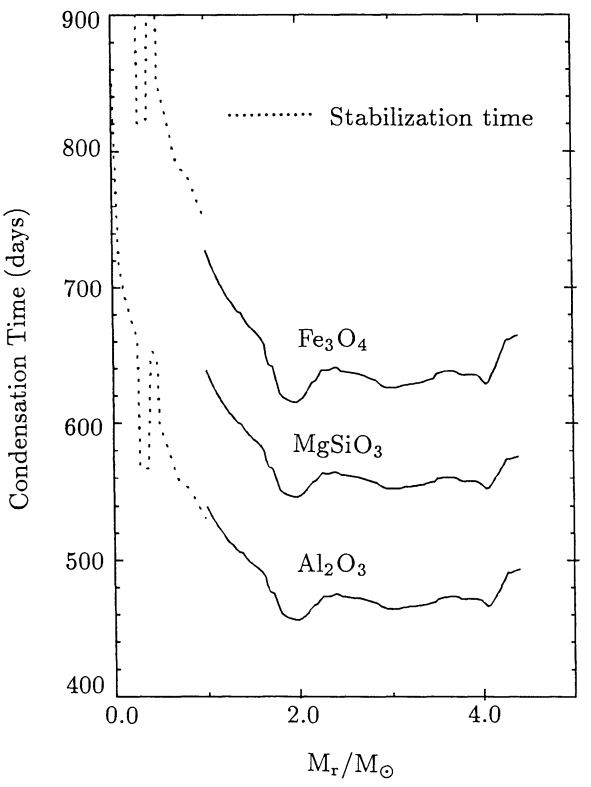

Fig. 4. The condensation time of each grain in the ejecta. The solid curves represent the *condensation time* determined by the process of homogeneous nucleation and grain growth, while the dotted curves represent the *stabilization time* of Al_2O_3 and Fe_3O_4 grains, after which dust grains grow stably against the heating due to the latent heat deposition during the grain growth

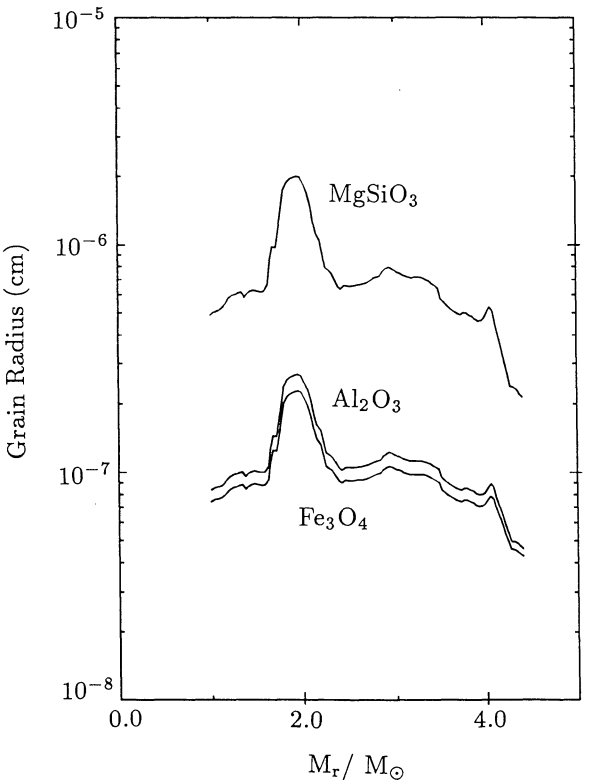

Fig. 5. The radii of dust grains formed in the region at $1.0\ M_\odot \leq M_r \leq 4.4\ M_\odot$ of the ejecta

that derived from the change in the decline rate of U, B, and V magnitude (Suntzeff & Bouchet 1990). The total mass of dust grains formed in this region is $\sim 0.23\ M_\odot$; $\sim 0.009\ M_\odot$ for Al_2O_3, $\sim 0.19\ M_\odot$ for $MgSiO_3$, and $\sim 0.031\ M_\odot$ for Fe_3O_4. The calculated grain radius smaller than 0.01 μm satisfies the constraint on the radius of dust grains in the ejecta, which is derived from the analysis of blue-shifted line profiles (Lucy et al. 1989). The radius of dust grains formed in the ejecta depends little on the parameter γ, so that the supernovae would be expected to be a major source of dust grains smaller than 0.01 μm by number in interstellar space. In this section, we discuss the result of calculations in comparison with the observational results.

4.1. The time evolution of the optical depth in the ejecta

The opacity in the visual to infrared region due to dust grains formed in the ejecta is dominated by the absorption of dust grains because $2\pi/\lambda \ll 1$ as seen from Fig. 5. The optical depth due to dust grains measured from the surface of grain formation region to a location of mass coordinate M_r at a time t is calculated by

$$\tau_\lambda(M_r, t) = \frac{1}{4t^2}\int_{M_r}^{M_s(t)} \kappa_\lambda(M_r', t)\frac{dM_r'}{v(M_r')^2}, \tag{1}$$

where $v(M_r)$ is the gas velocity at a location of M_r. The mass absorption coefficient of dust grains $\kappa_\lambda(M_r)$ is calculated by

$$\kappa_\lambda(M_r, t) = \sum_{i=1}^{3}\left(\frac{\beta_1 \pi r_0^3}{\mu m_H}\right)_i \left(\frac{r(t)}{r_\infty}\right)_i^3 \left(\frac{Q_{abs}}{r(t)}\right)_i, \tag{2}$$

where β_1 is relative number abundance of the key molecular species, μ mean molecular weight of gas, m_H hydrogen mass, and $Q_{abs}(\lambda, r)$ absorption efficiency factor. The subscript i denotes the grain species. The radius r_0 is an equivalent radius of the condensate per the key molecular species. The mean grain radius r_∞, which is calculated in the case that the key species is completely consumed, being introduced, the radius, of i-th grain species after the condensation time is given by the equation

$$\frac{1}{6}\ln\left|\frac{1-z^3}{(1-z)^3}\right| + \frac{2\sqrt{3}}{3}\left\{\tan^{-1}\left(\frac{2}{\sqrt{3}}z + \frac{1}{2}\right) - \frac{\pi}{6}\right\}$$
$$= \frac{1}{3}\left(\frac{r_0}{r_\infty}\right)\frac{t_{con}}{\tau_{coll,con}}\frac{2}{(1+3\gamma)}\left\{1 - \left(\frac{t}{t_{con}}\right)^{-(1+3\gamma)/2}\right\}, \tag{3}$$

where $z = r(t)/r_\infty$ and $\tau_{coll,con}$ is the collision time of the key molecular species at the condensation time.

Figure 6 shows the time evolution of the optical depths of the ejecta due to the grains newly formed in the ejecta at $\lambda = 0.55$ and 10 μm. The optical constants used for the calculation are taken from the tables of Toon & Pollack (1976) for Al_2O_3 and of Mukai (1989) for Mg-silicate and Fe_3O_4.

The optical depth $\tau_{0.55}$ at $\lambda = 0.55$ μm due to Al_2O_3 grains is less than 10^{-3}, while the optical depth τ_{10} at 10 μm is ~ 3. The mass absorption coefficient of Al_2O_3 grains is very small in the visual to near-infrared regions. As a result, the formation of Al_2O_3 grains starting from $\sim$day 460 is consistent with the observational result that there has been no observable change in the visual to near infrared regions in correspondence to the enhancement of 10 μm flux (Roche et al. 1989). Being accompanied by the formation of $MgSiO_3$ grains, the optical depths increase rapidly from $\sim$day 550 and reach $\tau_{0.55} \sim 1$ and $\tau_{10} \sim 1\,10^3$ at day 570. The optical depth $\tau_{0.55}$ again starts to

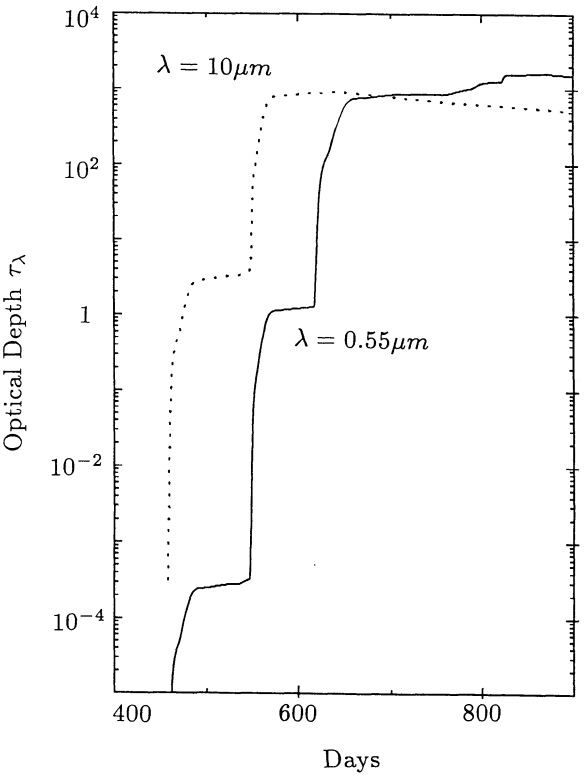

Fig. 6. The time evolution of the optical depths due to newly formed grains in the ejecta at the wavelengths of $\lambda = 0.55$ μm (solid curve) and 10 μm (dotted curve). The dust grain responsible for the optical depth is Al_2O_3 up to $\sim$day 550. The rapid increase of τ_{10} strating at $\sim$day 550 is due to the condensation of $MgSiO_3$ grains, and the rapid increase of $\tau_{0.55}$ starting at $\sim$day 620 is due to the condensation of Fe_3O_4 grains

increase rapidly from $\sim$day 620 up to $\tau_{0.55} \sim 1\,10^3$ at day 660 due to the formation of Fe_3O_4 grains. The effect of the formation of Fe_3O_4 grains on τ_{10} is not so remarkable because of the smaller abundance of Fe than that of Si. The gradual increase in $\tau_{0.55}$ after $\sim$day 770 is due to the contribution of Fe_3O_4 grains in the inner $1\ M_\odot$ region of the ejecta.

The analysis of the optical blue-shifted lines (Lucy et al. 1989, 1991) have shown that the extinction due to grains formed in the ejecta at $\lambda = 0.55$ μm is negligibly small up to day 530, increases rapidly after day 580 and gradually increases after day 670. This time evolution of optical depth in the ejecta can be explained qualitatively by the sequential condensation of Al_2O_3, $MgSiO_3$ and Fe_3O_4 grains in the ejecta. In the real ejecta, the thermal radiation from grains would lower the gas temperature in the ejecta more rapidly. This effect would lead to the earlier condensation of $MgSiO_3$ and Fe_3O_4 grains than those presented here.

It should be kept in mind that the optical constant of Mg-silicate adopted here (Mukai 1989) results in the absorption efficiency in the visual to near-infrared regions about three order of magnitude smaller than that calculated by using the optical constant of *astrophysical silicate* (Draine 1985). The optical depth $\tau_{0.55}$ due to $MgSiO_3$ grains is $\sim 1\,10^3$ times that shown in Fig. 6. if we use the optical constant of *astrophysical silicate.*

In the framework of our condensation calculations, the observational results relevant to the grain formation in the ejecta

are interpreted as follows: The enhancement of 10 μm flux at day 465 is due to the formation of Al_2O_3 grains, and the appearance of the blue-shifted line profiles due to the following formation of $MgSiO_3$ and Fe_3O_4 grains. Further the result of our calculation claims that the ejecta becomes optically thick in the visual to infrared region as a result of the formation of $MgSiO_3$ and Fe_3O_4 grains. Consequently the emergent radiation from the supernova would be dominated by the thermal radiation from the dust grains in the optically thick part of the ejecta. The photometric observations have confirmed that after ~day 600 most of the radiation from the supernova is dominated by the mid to far-infrared radiation and the energy spectra have been well fitted by the black-body curve (Wooden 1989; Suntzeff & Bouchet 1990), which is consistent with the thermal radiation from the dust grains in the optically thick part of the ejecta.

4.2. Condensation efficiency of dust grains and the degree of clumpiness in the ejecta

Contrary to the prediction based on the condensation calculation, the corrected optical depth at $\lambda = 0.55$ μm obtained from the analysis of the blue-shifted line profiles is very small in comparison with the calculated one after ~day 620: The derived $\tau_{0.55}$ from the analysis of [O I] line profiles is ~1.0 (Lucy et al. 1989), while the calculated $\tau_{0.55}$ reaches $\sim 1\,10^3$. The optical depth due to dust grains measured from the surface of the grain formation region at day 635 is shown in Fig. 7. Our results of calculations then suggest that at day 635 $\tau_{0.55}$ reaches ~1 at

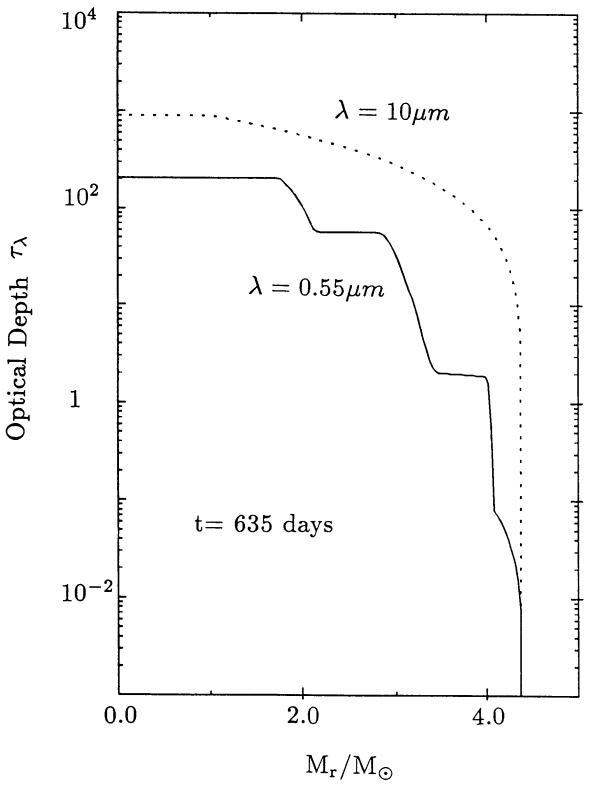

Fig. 7. The optical depths due to dust grains measured from the surface of grain formation region at day 635; the solid curve for $\tau_{0.55}$ and the dotted curve for τ_{10}

$M_r = 4.0\ M_\odot$ and that at $\lambda = 10$ μm the grain formation region in the ejecta is completely optically thick.

This discrepancy could be solved if the condensation efficiency of dust grains would be much smaller than $1 (\leq 1\,10^{-3})$, or if the ejecta would not be uniform and the grains would concentrate in the clumps as suggested by Lucy et al. (1991). The clumpy structure of the ejecta of SN 1987A have been also suggested from the analysis of the observed intensity of the Compton degraded X-rays (Kumagai et al. 1989) as well as the optical line profiles (Stathakis & Cannon 1988).

In this subsection, we attempt to estimate the condensation efficiency of dust grains and to investigate the degree and manner of clump in the ejecta from the thermal radiation from dust grains. We reproduce the observed 10 μm flux and compare the calculated total infrared luminosity from dust grains with the observed total infrared luminosity.

For simplicity, we assume that all grain species have the same temperature throughout the ejecta. The grain temperature T_{gr} is determined from the condition that the calculated 10 μm flux reproduces the observed one. In order to take account of the condensation efficiency of dust grains in the ejecta, we introduce the constant parameter $f_e (\leq 1)$ which reduces effectively the mass absorption coefficient as well as the emissivity of dust grains. For the degree of clumpiness of the ejecta, we adopt the model by Whitelock et al. (1989); the clumpy region occupies the solid angle x seen from the center of the supernova where the grain number density is $f_c (\geq 1)$ times that of the uniform ejecta, while the density in the other region is $1/f_c$ times that of the uniform ejecta. In this case, the flux of thermal radiation from dust grains at a given wavelength λ is calculated by

$$F_\lambda = \frac{1}{4D^2} \int_M \left\{ \frac{f_c}{f_c+1} \exp(-f_c \tau_\lambda) + \frac{1}{f_c+1} \exp(-\tau_\lambda / f_c) \right\} \times B_\lambda(T_{gr}) \kappa_\lambda(M'_r)\, dM'_r, \quad (4)$$

where B_λ is the Planck function. We adopt $D = 50$ kpc as the distance from the supernova, and assume that the parameters f_e and f_c are constant throughout the ejecta and are independent of time.

For the optically thin ejecta at 10 μm, the higher grain temperature is needed for smaller f_e and larger f_c to reproduce the observed 10 μm flux, and the resulting total infrared luminosity from dust grains increases. For the optically thick ejecta, on the other hand, the dependence of grain temperature on the parameters f_e and f_c is less than that of the total infrared luminosity from dust grains. Smaller f_e and larger f_c result in the smaller total infrared luminosity. The effect of the change in f_e and f_c on the calculated grain temperature is prominent for the optically thin ejecta at $\lambda = 10$ μm rather than for the optically thick ejecta. The resulting infrared luminosity for the optically thin ejecta is therefore sensitive to the change in f_e and f_c because the infrared luminosity strongly depends on the grain temperature.

Figures 8a and b show the calculated infrared light curve to be compared with the observations: Figure 8a is for the condensation efficiency of $f_e = 0.5$ and Fig. 8b for the clumpy ejecta of $f_c = 3$, where the open circles represent the observed 10 μm flux, the filled circles the observed infrared luminosity, and the open squares the calculated infrared luminosity. The total infrared luminosity and 10 μm flux are taken from Suntzeff & Bouchet (1990), where the observed 10 μm flux is evaluated from their tabulated values of total infrared luminosity and the effective

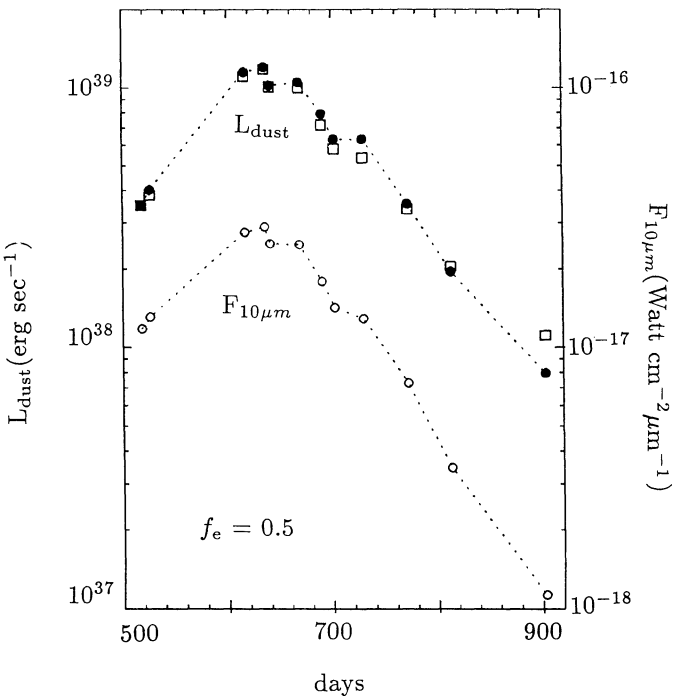

Fig. 8a. The comparison of the calculated total infrared light curve with the observed one for the condensation efficiency of $f_e = 0.5$. The infrared luminosity is calculated from the condition that the calculated 10 μm flux can reproduce the observed one. The open circles represent the observed 10 μm flux, the filled circles the observed total infrared luminosity, and the open squares the calculated one

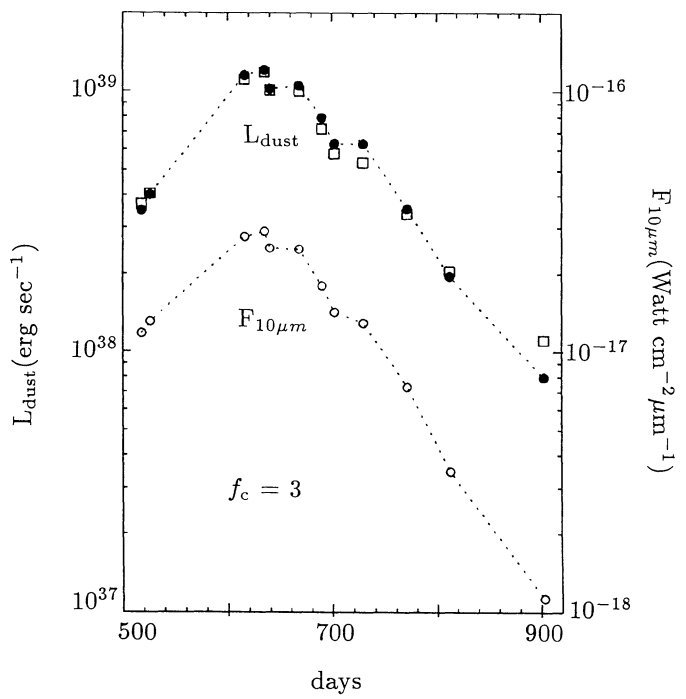

Fig. 8b. The same as Fig. 8a but for the clumpy ejecta of $f_c = 3$. Up to ~day 550 the total infrared luminosity attributes to the thermal radiation from Al_2O_3 grains, and afterwards the thermal radiation from $MgSiO_3$ grain dominates the total infrared luminosity, which is also true for Fig. 8a

temperature in order to compare the calculated total infrared luminosity with the observed one in a consistent manner. Note that in the calculations the contribution of free-free emission is subtracted before day 600 as suggested by Aitken et al. (1989) and Wooden (1989). For both cases, the calculated infrared light curve is in good agreement with the observed total infrared light curve except for day 903. In correspondence with the condensation times of each dust grain shown in Fig. 4, the grain species which attributes to the total infrared luminosity is Al_2O_3 grains up to ~day 550. Afterwards, the thermal radiation from $MgSiO_3$ grains dominates the total infrared luminosity. For $f_e < 0.3$ and $f_c > 5$, the agreement between the calculated and the observed total infrared light curve is poor when the constraint is given from the observed 10 μm flux. Figure 9, for example, shows the calculated infrared light curve for $f_c = 30$. The disagreement between the observed infrared luminosity and the calculated one is most remarkable around day 520 because the ejecta is optically thin at $\lambda = 10$ μm, which is true for smaller f_e. The results of our calculations then suggest either the condensation efficiency $f_e \geq 0.3$ or the degree of clumpiness $f_c \leq 5$ in the ejecta.

The constraint on the condensation efficiency $f_e > 0.3$ would be inconsistent with the interpretation of the blue-shifted line profiles with $f_e \leq 10^{-3}$. It therefore seems more likely that the discrepancy between the observations and the theoretical prediction is due to the clumpy structure in the ejecta. Lucy et al. (1991) also have suggested the clumpy structure in the ejecta, paying attention to the degree of the decrease in the intensity of [Si I] line

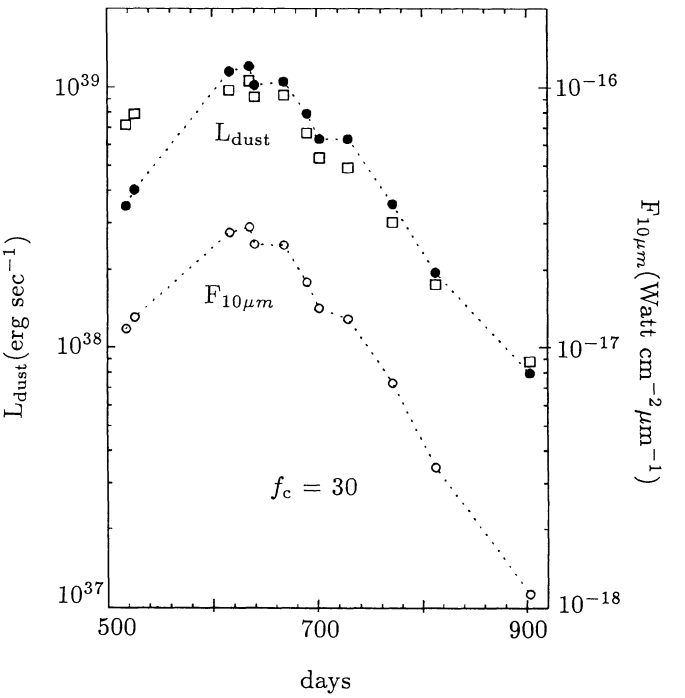

Fig. 9. The calculated infrared light curve for $f_c = 30$. The disagreement between the observed total infrared luminosity and the calculated one is most remarkable for the optically thin ejecta at $\lambda = 10$ μm around day 520. The reason is explained as the followings: When the ejecta is not extremely optically thick at $\lambda = 10$ μm, the higher grain temperature is needed for larger f_c and smaller f_e to reproduce the observed 10 μm flux. The resulting total infrared luminosity then becomes higher because the total infrared luminosity strongly depends on the grain temperature

concurrently occurred with the appearance of the blue-shifted line profiles and to the behavior of derived extinction curve.

The constraint $f_c \geq 5$, which is obtained from condition that the infrared light curve is to be consistent with the observed 10 μm flux, implies that the clumpy region occupies the fraction of at least ~20% in the ejecta on the average, and that the ratio of the grain number density in the clumps to that in the intervening regions is less than 25. For $f_c = 5$, for example, the intervening region is optically thin at $\lambda = 0.55$ μm up to ~day 620. Afterwards, the condensation of Fe_3O_4 grains makes the intervening region optically thick. The optical depth of the intervening region at $\lambda = 0.55$ μm reaches ~1 at $M_r \sim 3.3\ M_\odot$ at day 635 as seen from Fig. 7, and at $M_r \sim 4.2\ M_\odot$ at day 670. Up to ~day 690, even the intervening region entirely becomes optically thick at the visual wavelength. The result of our calculation then suggests that the time development of optical depth derived from the analysis of blue-shifted line profiles reflects not only the condensation episode in the ejecta but also the resulting change of the locations of line emitting region.

The grain temperature, for example, are about 430 K at day 518, 420 K at day 635, 340 K at day 702, and 240 K at day 813 for $f_c = 3$, which is in reasonable agreement with the grain temperature derived from the observations by Roche et al. (1989) at around day 520, and by Suntzeff & Bouchet (1990) after day 600. Also the energy distribution of the resulting thermal radiation is black-body after day 600, being consistent with the observations (Wooden 1989; Suntzeff & Bouchet 1990). Our conclusion is almost independent of the optical constants adopted for Mg-silicate grains. With the use of the optical constant tabulated by Draine (1985) we also obtain the constraint of $f_c \leq 5$ in order to reproduce the observed total infrared luminosity.

If $f_c \leq 5$, the supernova core, i.e., the inner 4.4 $M_\odot$ region of the ejecta, is essentially blacked out with dust grains by ~day 700. The entire supernova is not blacked out, however, since a significant fraction of radioactive elements exist and provide energy source for the emission of U to M bolometric light curve from the outer envelope. In other words, L_{U-M} originates from the envelope, while L_{IR} is emitted from the core. This interpretation is consistent with the fact that L_{U-M} have decreased in proportional to $L_{CO} - L_{X_\gamma}$ after ~day 670 (Whitelock et al. 1989) as well as the fact that the rapid decline of U, B and V magnitude have stopped by day 700 (Suntzeff & Bouchet 1990).

5. Concluding remarks

The formation of dust grains have been reinvestigated on the basis of the revised hydrodynamical model and the abundance distribution of the ejecta. The theory of homogeneous nucleation and grain growth results in the sequential formation of Al_2O_3, $MgSiO_3$ and Fe_3O_4 grains respectively in the region at $1.0\ M_\odot \leq M_r \leq 4.4\ M_\odot$ of the ejecta. In the inner region at $M_r \leq 1.0\ M_\odot$ the latent heat deposition during grain growth retards the formation of dust grains, whose effect is most prominent for $MgSiO_3$ grains.

The duration of grain formation in the region at $1.0\ M_\odot \leq M_r \leq 4.4\ M_\odot$ (from ~day 460 to ~day 730) derived from the calculation is comparable to that estimated from the analysis of blue shifted-line profiles and that from the change in the decline rate of U, B, and V magnitude. The total mass of dust grains formed in this region is $\sim 0.23\ M_\odot$. The radii of grains formed in the ejecta are typically ~10 Å for Al_2O_3 and Fe_3O_4 grains, and ~70 Å for $MgSiO_3$ grains. Formation of these sized grains in the ejecta satisfies the constraint on the grain radius derived from the analysis of the blue-shifted line profiles. Thus supernovae are considered to be a major source of small dust grains in interstellar space, which are required to explain the rapid increase of interstellar extinction curve in UV region.

The sequential formation of Al_2O_3, $MgSiO_3$ and Fe_3O_4 grains in the ejecta would be able to explain qualitatively the behavior of the time development of the extinction in the ejecta obtained from the analysis of the blue-shifted line profiles. The light curve of the calculated total infrared luminosity based on the condensation calculation and the observed 10 μm flux is in good agreement with the observed curve when the condensation efficiency of dust grains is greater than 0.3 or when clumps occupies the fraction of at least ~20% in the ejecta. When the eject is clumpy with the degree of $f_c \leq 5$, the supernova core (i.e., inner 4.4 $M_\odot$ region of the ejecta) is blacked out with dust grains by ~day 700. This is consistent with the behavior of U to M bolometric light curve and with the change in the decline rate of U, B and V magnitude. The observed infrared radiation arises from the grains in the optically thick part of the ejecta after day 620.

Acknowledgements. The authors thank Dr. C. Dominik, the referee, for helpful comments and discussions on improving the manuscript. The authors also would like to thank Dr. T. Shigeyama for useful discussion, and Dr. T. Onaka for his information. One of the authors, T.K., is greatful to Prof. H. Fechtig and Prof. H.J. Völk for their hospitality during his stay at Max-Plank-Institut für Kernphysik. The numerical calculations were performed by VAX-station 2000 at MPIK. This work has been supported in part by the Grant-in-Aid for Scientific Research (02234202, 02302024, 03218202) of the Japanese Ministry of Education.

References

Aitken D.K., Smith C.H., James S.D., Roche P.F., Hyland A.R., McGregor P.J., 1988, MNRAS 235, 19
Burki G., Gramer N., Burnet M., Rufener F., Pernier B., Richard C., 1989, A&A 213, L26
Catchpole R.M., et al., 1987, MNRAS 229, 15
Catchpole R.M., et al., 1988, MNRAS 231, 75
Danziger I.J., Bouchet P., Gouiffes C., Rufener F., 1988, in: Big Bang, Active Galactic Nuclei and Supernovae, eds. S. Hayakawa, K. Sato, Universal Academic Press, Tokyo, p. 429
Danziger I.J., Gouiffes C., Bouchet P., Lucy L.B., 1989, IAU Circ., No. 4746
Draine B.T., Salpeter E.E., 1977, J. Chem. Phys. 67, 2230
Draine B.T., 1985, ApJS 57, 587
Dwek E., 1983, ApJ 274, 175
Dwek E., 1988, ApJ 329, 814
Dwek E. et al., 1983, ApJ 274, 168
Hasegawa H., Kozasa T., 1988, Prog. Theor. Phys., Suppl. 96, 107
Hashimoto M., Nomoto K., Shigeyama T., 1989, A&A 210, L5
Kozasa T., Hasegawa H., 1987, Prog. Theor. Phys. 77, 1402
Kozasa T., Hasegawa H., Nomoto K., 1989a, ApJ 344, 325 (Paper I)
Kozasa T., Hasegawa H., Nomoto K., 1989b, ApJ 346, L81
Kumagai S., Shigeyama T., Nomoto K., Itoh M., Nishimura J., Tsuruta S., 1989, ApJ 345, 412

Lucy L.B., Danziger I.J., Gouiffes C., Bouchet P., 1989, in: Structure and Dynamics of Interstellar Medium, IAU Colloq. No. 120, eds. G. Tenorio-Tagle, M. Mole, J. Melnick, Springer, Berlin Heidelberg New York, p. 164
Lucy L.B., Danziger I.J., Gouiffes C., Bouchet P., 1991, in: Supernovae, ed. S.E. Woosley, Springer, New York Berlin Heidelberg, p. 82
Moseley S.H., Dwek E., Glaccum J.R., Loewenstein R.F., Silbersberg R.F., 1989, Nat 340, 697
Mukai T., 1989, in: Evolution of Interstellar Dust and Related Topics, eds. A. Bonetti, J.M. Greenberg, S. Aiello, Elsevier, North-Holland, Amsterdam, p. 397
Donn B., Nuth J., 1985, ApJ 288, L187
Roche P.F., Aitken D.K., Smith C.H., James S.D., 1989, Nat 337, 533
Shigeyama T., Nomoto K., 1991, ApJ 360, 242
Smith C.H., 1989 (private communication)
Stathakis R., Cannon R.D., 1988, AAO Newsletter 45
Suntzeff N.B., Bouchet P., 1990, AJ 99, 650
Thielemann F.K., Hashimoto M., Nomoto K., 1990, ApJ 349, 222
Toon O.B., Pollack J.B., 1976, J. Geophys. Res. 81, 5733
Whitelock P.A., et al., 1989, MNRAS 240, 7
Wooden D.H., 1989, Ph.D. thesis. Univ. of California Santa Cruz
Yamamoto T., Hasegawa H., 1977, Prog. Theor. Phys. 58, 816